# INFLUENCE OF THE INTERFACE BONDING STRENGTH ON BRITTLE CRACK PROPAGATION IN BI-MATERIAL STRUCTURAL COMPONENTS

Alberto Carpinteri, Marco Paggi
Department of Structural and Geotechnical Engineering, Politecnico di Torino
C.so Duca degli Abruzzi 24 – 10129 Torino, Italy
alberto.carpinteri@polito.it marco.paggi@polito.it

## Abstract

The influence of the interface bonding strength on brittle crack propagation in bi-material structures is investigated. In this study a crack is set at the vertex of the interface between two joined dissimilar materials. Competition between several possible crack trajectories is endeavoured, paying special attention to the effect of thermo-elastic and residual stresses on crack propagation.

## Introduction

Bi-material structural components are commonly encountered in a variety of engineering applications, such as wear resistant materials, microelectronic devices and composite laminates used in aircraft structures. During the manufacturing process, interphases having material properties intermediate between those of the material constituents are developed [1,2]. As a result, the mechanical behavior and the overall performance of the component are not limited by the bulk properties, but by the interface characteristics. In fact, according to Linear Elastic Fracture Mechanics, if a system consisting of two edge-bonded elastic wedges of different materials is considered (see Fig. 1), a stress-singularity is present at the vertex of the bi-material interface, even in the absence of a re-entrant corner [3]. The power of this stress-singularity depends both on the elastic bi-material mismatch parameters [4], and on the wedge geometry. From the practical point of view, the existence of such a stress-singularity means that microfailure processes due to initial defects are likely to occur at the interfaces.

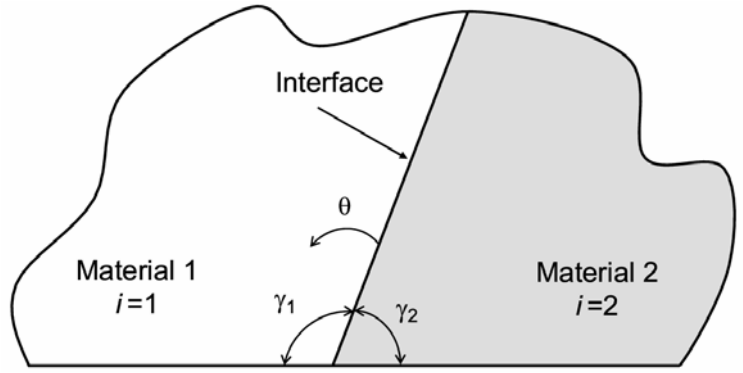


FIGURE 1. Scheme of two edge-bonded elastic wedges.

Furthermore, an additional complexity arising in many interface problems is provided by significant residual and/or thermo-elastic stresses present in the region close to the interface. The residual stress field is due to the bonding process and it is caused by the different

expansion coefficients of the two constituent materials and by the elastic mismatch. On the other hand, many engineering components experience thermal loads during their life and significant thermo-elastic stresses have to be taken into account [5]. Hence, the applied thermal loads, together with the mechanical forces acting on the structure, may result in a crack enucleation and growth with initial position close to the bi-material interface.

By considering an initial crack which enucleates from the bi-material interface, the problem of brittle crack propagation in bi-material structural components is addressed. The external load is not set *a-priori* in the numerical analyses, but it is computed at each step by enforcing the condition for crack propagation [6]. In this way, stable or unstable crack propagations can be easily controlled. To be more specific, the conditions for pure delamination along the bi-material interface, or for deflection into one of the material regions, are given by a strain energy release rate based failure criterion. In other words, we assume that the crack propagates in the direction where it is more suitable to propagate from an energy point of view. As a result, the competition between the different failure modes or crack trajectories can be readily recognized and expressed in terms of the mechanical properties of the interface. In this framework, thermo-elastic and residual stress fields are superimposed to the mechanical ones and their effect on brittle crack propagation is carefully investigated. Detailed numerical examples concerning engineering problems are provided.

## Singular points in joined dissimilar materials under mechanical and thermal loading

According to Linear Elastic Fracture Mechanics, a stress singularity exists at the vertex of the interface between two joined dissimilar materials (Fig. 1). Investigations on the order of the stress singularity arising from this type of joint geometry under mechanical and thermal loading were provided by Bogy [3], Bogy and Wang [7], Hein and Erdogan [8], and Yang and Munz [9], among others.

According to Williams [10], it is possible to assume, for the *i*-th subregion (Fig.1), the following separable form for the biharmonic stress function $\Phi_i$:

$$\Phi_i(r,\theta) = \sum_j r^{\lambda_j + 1} f_{i,j}(\theta, \lambda_j) \tag{1}$$

where $\lambda_j$ and $f_{i,j}$ are referred to as eigenvalues and eigenfunctions, respectively.

The summation with respect to index *j* is introduced in Eq. (1), since it is possible to have more than one eigenvalue for each problem. For $0<\mathrm{Re}\lambda_j<1$, the biharmonic condition requires $f_i$ to be of the form:

$$f_{i,j}(\theta,\lambda_j) = A_{i,j}\sin(\lambda_j+1)\theta + B_{i,j}\cos(\lambda_j+1)\theta + C_{i,j}\sin(\lambda_j-1)\theta + D_{i,j}\cos(\lambda_j-1)\theta, \tag{2}$$

where $A_{i,j}$, $B_{i,j}$, $C_{i,j}$ and $D_{i,j}$ are undetermined constants. For the particular case of $\mathrm{Re}\lambda_j=1$, the stress term becomes independent of the distance *r* and, according to Yang and Munz [9], an additional term has to be added to Eq.(1):

$$\Phi_{i,0}(r,\theta) = r^2\left[E_{i,0}\theta + F_{i,0} + G_{i,0}\sin(2\theta) + H_{i,0}\cos(2\theta)\right]. \tag{3}$$

The stress field can be computed from Eqs.(1) and (3) as follows:

$$\sigma^{i}_{r} = \frac{1}{r}\frac{\partial \Phi}{\partial r} + \frac{1}{r^2}\frac{\partial^2 \Phi}{\partial \theta^2}$$
$$\sigma^{i}_{\theta} = \frac{\partial^2 \Phi}{\partial r^2} \qquad (4)$$
$$\tau^{i}_{r\theta} = -\frac{\partial}{\partial r}\left(\frac{1}{r}\frac{\partial \Phi}{\partial \theta}\right)$$

Introducing the relationships between strains and displacements in polar coordinates and the constitutive equations, the displacements under mechanical and thermal loadings can be computed (see [9] for more details). It is important to notice that the displacement field depends both on the shear moduli $G_i$, and on the product between the thermal expansion coefficients $\alpha_i$ and the temperature excursion $\Delta T$ to which the elements are exposed. Imposed boundary conditions permit then to compute the order of the stress-singularity and to determine the singular and the regular stress components. For this problem, four stress-free conditions along the free edges and four stress and displacement continuity conditions across the bi-material interface have to be taken into account:

$$\begin{aligned}
&\sigma_{\theta}^{1}(r,\gamma_1) = 0 && \sigma_{\theta}^{1}(r,0) = \sigma_{\theta}^{2}(r,0)\\
&\tau_{r\theta}^{1}(r,\gamma_1) = 0 && \tau_{r\theta}^{1}(r,0) = \tau_{r\theta}^{2}(r,0)\\
&\sigma_{\theta}^{2}(r,\gamma_2) = 0 && u_{r}^{1}(r,0) = u_{r}^{2}(r,0)\\
&\tau_{r\theta}^{2}(r,\gamma_2) = 0 && u_{\theta}^{1}(r,0) = u_{\theta}^{2}(r,0)
\end{aligned} \qquad (5)$$

This eight linear equations system can be solved by splitting it into two groups of equations. Firstly, by considering the terms which depend on the distance $r$, a system of 8 equations in 9 unknowns $A_{i,j}$, $B_{i,j}$, $C_{i,j}$, $D_{i,j}$, and $\lambda_j$, can be symbolically written as:

$$\Lambda \mathbf{v} = \mathbf{0}, \qquad (6)$$

where $\Lambda$ denotes the coefficient matrix which depends on $\lambda_j$, and $\mathbf{v}$ represents the vector which collects the unknowns $A_{i,j}$, $B_{i,j}$, $C_{i,j}$, $D_{i,j}$. A nontrivial solution to the system exists only if the determinant of the coefficient matrix vanishes. This yields to a characteristic equation which has to be solved for eigenvalues $\lambda_j$ which are in general complex. Seeking for $0 < \mathrm{Re}\lambda_j < 1$, the order of the stress-singularity and the corresponding singular stresses can be computed. They are independent of thermal loading and, for different geometrical and material combinations, asymptotic solutions were early provided by Bogy [3].

Eventually, a second system can be obtained from the terms in Eq. (5) which are independent of $r$. The solution to this system allows to obtain the coefficients $E_{i,0}$, $F_{i,0}$, $G_{i,0}$, $H_{i,0}$ of the regular stresses which have to be superimposed to the singular stress field. As observed by Munz et al. [11], in the case of vanishing singular stress exponent, i.e. for $\lambda_j=1$, the regular term tends to infinity due to the difference in the thermal expansion coefficients of the two materials. This result implies that the regular term can be extremely significant and it can provide an important contribution to the interface normal stress distribution for cases of weak material mismatch leading to $\lambda_j \cong 1$.

## Competition between thermo-elastic and residual stresses

Multi-layered elements used for mechanical and electronic applications are usually subjected to nonuniform temperature distributions during their life and the solution of a preliminary steady-state thermal problem is required to estimate the temperature distribution within the

structural elements. Residual stresses are instead generated during the bonding process and are usually caused by a uniform temperature distribution. From the theoretical point of view, it is important to notice that the problem of residual stresses induced by an hot bonding of two material components during the fabrication process can be considered equivalent, neglecting the algebraic sign, to the problem of thermal stresses induced by a temperature increase in a bonded two-material structure. As a consequence, the problem of residual stresses induced in the elemnts by a temperature increase $\Delta T$ can be studied as the problem of thermal stresses due to a temperature decrease $-\Delta$T. As a result, the competition between residual and thermo-elastic stresses is favorable, since these stress fields can be completely compensated when the bi-material elements are subjected to the same temperature excursion and distribution as that applied during fabrication. This implies that the critical conditions for these components are usually attained during the first stage of their life, when residual stresses are prevailing. On the other hand, only a partial compensation can be obtained when the temperature distribution during the normal use does not match exactly that due to the bonding process.

## Competition between crack deflection and delamination at a bi-material interface

When a crack grows at the interface between two different materials, two possibilities may occur during propagation: to continue to grow along the interface giving rise to a pure delamination, or to move out of the interface into one of the two material regions. In the sequel we assume that the interface, like a continuum, presents a resistance to cracking, i.e. a critical interface fracture energy $\Gamma^{i}_{IC}$. According to He and Hutchinson [12] and to He et al. [13], the conditions for pure delamination along the bi-material interface, or for deflection into one of the material regions can be stated using a strain energy based failure criterion. By considering the ratio between the strain energy release rate for delamination and the critical interface fracture energy, $\Gamma_{del}/\Gamma^{i}_{IC}$, and the ratio between the strain energy release rate for crack deflection into one of the constituent materials and the corresponding critical strain energy release rate, $\Gamma_{def}/\Gamma_{IC}$, the crack continues to propagate along the interface if:

$$\frac{\mathcal{G}_{del}}{\mathcal{G}_{IC}} > \frac{\mathcal{G}_{def}}{\mathcal{G}_{IC}}, \tag{7}$$

otherwise it deflects into one of the neighborhood materials.

This failure criterion has been implemented in the FEM code FRANC2D by Ingraffea and Wawrzynek [6], developing the following propagation algorithm:

(1) for each material region around a crack-tip:
- find the direction of the maximum tensile circumferential stress;
- remesh to add a finite crack increment in this direction;
- solve the resulting finite element equations;
- normalize the global change in strain energy with respect to the crack increment and compute the ratio with the critical energy release rate.

(2) For each interface around the crack-tip:
- extend the crack a finite distance along the interface;
- solve the resulting finite element equations;
- use the relative opening and sliding at the crack-tip to determine the load angle and the critical strain energy release rate;
- normalize the change in strain energy with respect to the crack increment and find the ratio with the critical strain energy release rate.

(3) The direction of propagation is that with the largest associated ratio of the rate of energy

release to the critical rate of energy release.

## Numerical examples

In this section the competition among several crack trajectories of an interface crack is investigated. As a typical example, we consider a bi-layered element composed of a hard metal substrate and a wear-resistant external layer, widely used for rock drilling as detailed described in [14]. A steel support completes the tool and mechanical properties of the constituent materials can be found in [15,16]. Due to the difference in thermal expansion coefficients and mechanical properties of the two layers, as the temperature decreases after bonding, a residual compressive stress is set up in the external layer and a residual tensile stress in the hard metal substrate. This residual stress increases when the temperature falls, whereas when the temperature rises, as it occurs during drilling, high tensile stresses are induced in the external layer and a reduction of residual stresses should be expected.

In order to verify these assumptions, a uniform temperature distribution due to bonding is superimposed to the nonuniform temperature distribution experienced during the normal use of the tool. The former distribution assumes a temperature variation equal to $\Delta T$=–500°C, whereas the latter is estimated by performing a preliminary steady-state thermal analysis with a temperature increment equal to $\Delta T$=500°C localized at the tool tip. Residual tangential stresses along the interface, $\tau^{RES}$, thermo-elastic stresses, $\tau^{TH}$, and total tangential stresses are depicted in Fig. 2.

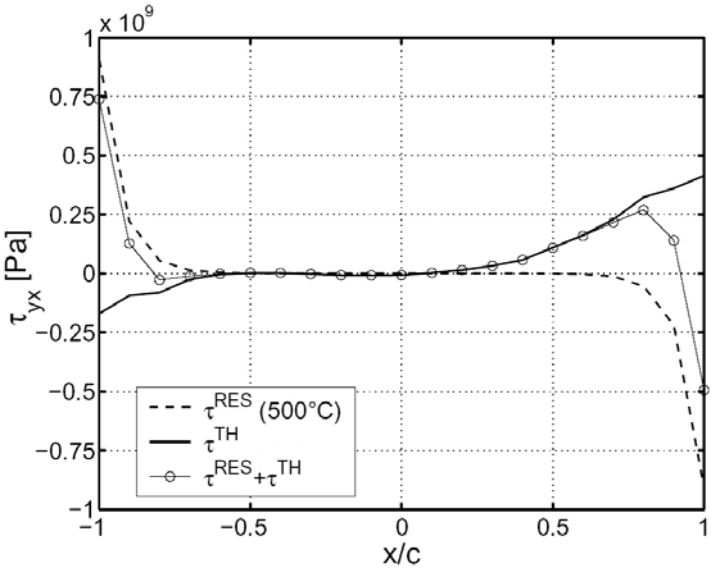


FIGURE 2. Tangential stress along the interface.

The parameter *x/c* denotes the relative position along the interface and the intersection of the interface with the free-edges of the bi-layered element is obtained for *x/c*=1. The tangential residual stress at the interface is symmetric and reaches its maximum value at the free ends. Thermo-elastic stresses present an opposite sign with respect to the residual ones and a lack of symmetry due to the nonsymmetric temperature distribution in the tool can be observed. At the free edges the residual stress prevails with respect to the thermal one and, thanks to the competition, a reduction by one third of the residual tangential stress occurs. As

previously discussed, the stress is globally negligible in the remaining points along the interface (see also the dotted line in Fig. 2).

After this preliminary analysis, a crack whose initial length is set equal to that of existing defects is introduced at the vertex of the interface between the two joined layers. An impact force is then applied at the tip of the tool in the vertical direction. Experiments showed that this loading condition can produce either a crack deflection into the external layer, referred to as *gross fracturing*, or a pure delamination along the interface [14].

From numerical investigations, we observe that only a competition between delamination or deflection into the external layer are real possibilities, whereas deflection into the hard metal is not permitted due to its high fracture toughness. Furthermore, we observe that brittle crack propagation along the interface can occur only if the interface toughness is less than approximately one third of that of the external layer. Assuming the limit case of a weak interface, brittle delamination is simulated and the deformed meshes are shown in Fig. 3. The magnitude of the external load is not set *a-priori*, but it is computed at each step by enforcing the condition for crack propagation [6].

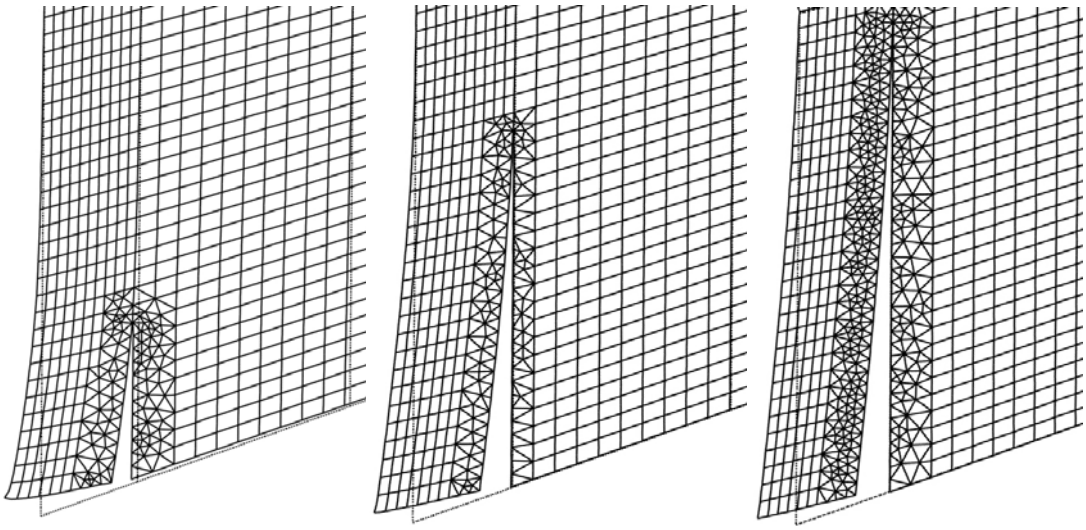

FIGURE 3. Deformed meshes corresponding to three steps of delamination.

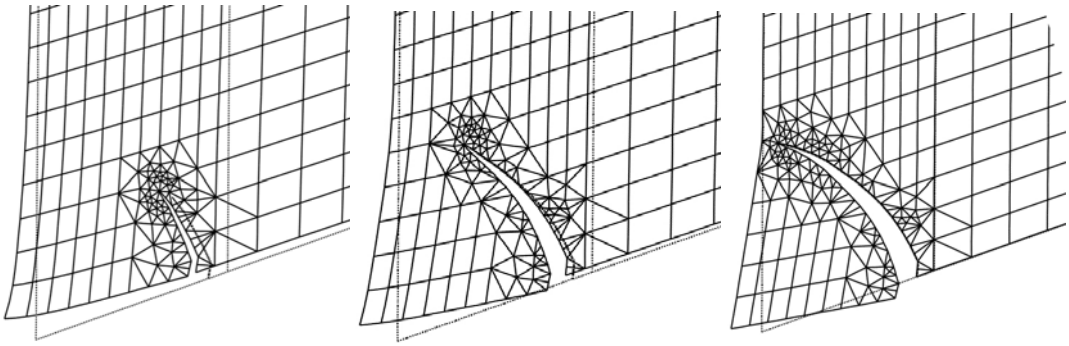

FIGURE 4. Deformed meshes corresponding to three steps of gross fracturing.

On the other hand, by assuming a normal interface, i.e. the interface toughness has an intermediate value with respect to those of the neighbourhood materials, a deflection into the external layer is simulated. Deformed meshes during crack propagation are shown in Fig. 4.

In both case studies, the nondimensional external load for crack propagation, $P_c/P_{c,0}^{GF}$, is computed at each step and depicted in Fig. 5 in terms of the nondimensional crack length, $a/a_{max}$. Critical loads for crack propagation in the absence of thermo-elastic and residual stress fields are also shown in the same diagrams for each failure mode (see dashed lines). In these pictures $P_{c,0}^{GF}$ represents the critical load for crack propagation and it corresponds to the initial crack length $a_0$ for the gross-fracturing failure mode with mechanical load only. Parameter $a_{max}$ denotes the maximum crack length for each failure mode corresponding to a broken external layer for gross fracturing, and to the total interface length in the case of pure delamination, respectively. It has to be noticed that unstable crack propagations take place in both failure modes, since the external load has to be reduced at each step. In spite of the fact that the crack trajectories with or without thermo-elastic and residual stress fields are approximately the same, the critical load for crack propagation is significantly influenced by their presence. In the case of gross-fracturing it is reduced by a factor of two, whereas that corresponding to delamination is slightly increased.

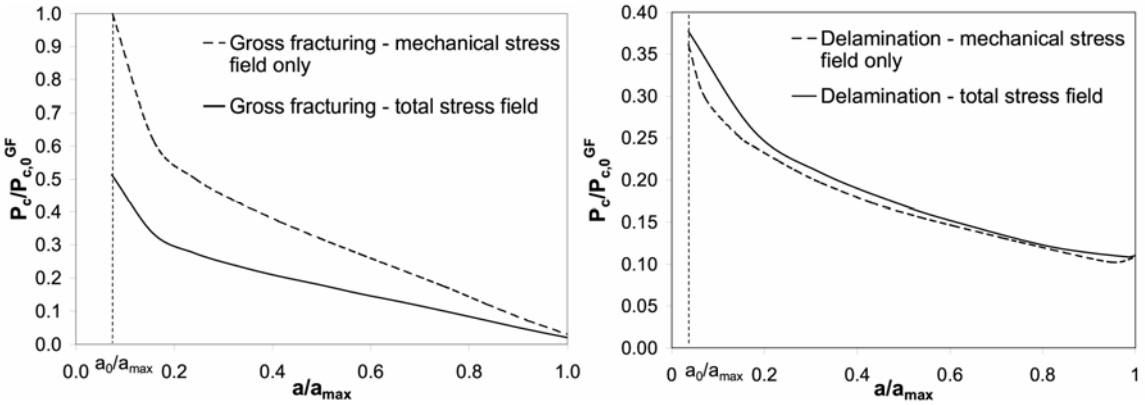


(a) (b)

FIGURE 5. Nondimensional critical load vs. nondimensional crack length: (a) delamination and (b) gross fracturing.

Eventually, the competition between the failure modes can be studied by comparing the evolution of the critical loads corresponding to the total stress field depicted in Figs. 5a,b. As previously observed, for this particular case study gross-fracturing prevails with respect to delamination in the case of normal interfaces. On the contrary, when the interface is extremely weak, the non-dimensional critical load for delamination is less than that for gross fracturing and crack propagation along the interface should prevail with respect to a crack deflection inside the external layer.

## Discussion and conclusions

The mechanical behavior of advanced structures composed by several materials is strongly influenced by damage phenomena occurring at the interfaces. These problems have a considerable importance in traditional structural elements, as well as in new-conception structured materials used in electronic devices and cutting tools. Therefore, tailoring of well-bonded, durable interfaces between the constituent materials has become a critical concern.

Durability is a primary issue since important factors, such as temperature and residual stresses to which the material is subjected, can degrade interfacial adhesion as well as the properties of the constituent phases. From the asymptotic analysis presented in the first section, it is well-known that stress-singularities occur at the vertex of the interface between two joined dissimilar materials. These singularities lead to crack enucleation in brittle materials and little attention has been spent in the Literature to the problem of crack propagation. In the present paper the influence of the interface bonding strength on brittle crack propagation in bi-material elements is addressed. Competition between different crack trajectories, or failure modes, was deeply investigated. For the presented case study, it is shown that thermo-elastic and residual stresses play a fundamental role and have to be carefully taken into account in order to have a satisfactory description of the real phenomenon.

## Acknowledgements

The present research work was carried out with the financial support of the Italian Ministry of University and Scientific Research (MIUR).

## References

1. Kakavas, P.A., Anifantis, N.K. and Papanicolaou, G.C., *Composites Part A*, vol. **29A**, 1021-1026, 1998.
2. Mukherjee, S., Ananth, C.R. and Chandra, N., *Composites Part A*, vol. **29A**, 1213-1219, 1998.
3. Bogy, D.B., *J. Appl. Mech.*, vol. **38**, 377-386, 1971.
4. Dundurs, J., In *Mathematics of Dislocation*, edited by T. Mura, ASME, New York, 1969, 70-115.
5. Rodriguez, M.P. and Shammas, N.Y.A., *Microelectronics Reliability*, vol. **41**, 517-523, 2001.
6. Ingraffea, A.R. and Wawrzynek, P.A., *Discrete modeling of crack propagation: theoretical aspects and implementation issues in two and three dimensions*, School of Civil and Environmental Engineering, Cornell University, Report No. 91-5, 1991.
7. Bogy, D.B. and Wang, K.C., *Int. J. Solids Structures*, vol. **7**, 993-1005, 1971.
8. Hein, V.L. and Erdogan, F., *Int. J. Fract. Mech.*, vol. **7**, 317-330, 1971.
9. Yang, Y.Y. and Munz, D., *Int. J. Solids Structures*, vol. **34**, 1199-1216, 1997.
10. Williams, M.L., *J. Appl. Mech.*, vol. **74**, 526-528, 1952.
11. Munz, D., Fett, T. and Yang, Y.Y., *Engng. Fract. Mech.*, vol. **44**, 185-194, 1993.
12. He, M.Y. and Hutchinson, J.W., *Int. J. Solids Structures*, vol. **25**, 1053-1067, 1989.
13. He, M.Y., Evans, A.G. and Hutchinson, J.W., *Int. J. Solids Structures*, vol. **31**, 3443-3455, 1994.
14. Lin, T.P., Hood, M., Cooper, G.A. and Li, X., *Wear*, vol. **156**, 133-150, 1992.
15. Ravichandran, K.S., *Acta Metall. Mater.*, vol. **42**, 143-150, 1994.
16. Lammer, A., *Mater. Sci. Tech.*, vol. **4**, 949-955, 1988.